Research Article

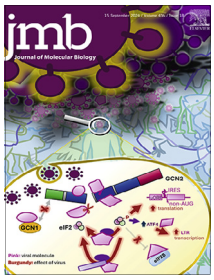

RNase R Affects the Level of Fatty Acid Biosynthesis Transcripts Leading to Changes in membrane Fluidity

André Filipe Alípio [a,†], Cátia Bárria [a,*,†], Vânia Pobre [a], Ana Rita Matos [b], Sara Carrera Prata [a], Mónica Amblar [c], Cecília Maria Arraiano [a] and Susana Domingues [a,*]

***a* - Instituto de Tecnologia Química e Biológica António Xavier,** *Universidade Nova de Lisboa, Av. da República, 2780-157 Oeiras, Portugal*

***b* - BioISI – Biosystems and Integrative Sciences Institute,** *Environmental and Molecular Plant Physiology Laboratory, Departamento de Biologia Vegetal, Faculdade de Ciências da Universidade de Lisboa, Campo Grande, 1749-016 Lisboa, Portugal*

***c* - Unidad de Patología Molecular del Neumococo,** *Centro Nacional de Microbiología, Instituto de Salud Carlos III. Majadahonda, Madrid 28220, Spain*

Correspondence to Cátia Bárria and Susana Domingues: *catiabarria@itqb.unl.pt (C. Bárria), susanadomingues@itqb.unl.pt (S. Domingues)*

https://doi.org/10.1016/j.jmb.2024.168711

Edited by Philip C. Bevilacqua

Abstract

Previous studies on RNase R have highlighted significant effects of this ribonuclease in several processes of *Streptococcus pneumoniae* biology. In this work we show that elimination of RNase R results in overexpression of most of genes encoding the components of type II fatty acid biosynthesis (FASII) cluster. We demonstrate that RNase R is implicated in the turnover of most of transcripts from this pathway, affecting the outcome of the whole FASII cluster, and ultimately leading to changes in the membrane fatty acid composition. Our results show that the membrane of the deleted strain contains higher proportion of unsaturated and long-chained fatty acids than the membrane of the wild type strain. These alterations render the RNase R mutant more prone to membrane lipid peroxidation and are likely the reason for the increased sensitivity of this strain to detergent lysis and to the action of the bacteriocin nisin. Reprogramming of membrane fluidity is an adaptative cell response crucial for bacterial survival in constantly changing environmental conditions. The data presented here is suggestive of a role for RNase R in the composition of *S. pneumoniae* membrane, with strong impact on pneumococci adaptation to different stress situations.

Introduction

Streptococcus pneumoniae is an important human respiratory pathogen that causes a variety of serious diseases. It is an opportunistic pathogen commonly found in the nasopharynx flora of healthy individuals. Pneumococcal colonization usually occurs on the mucosal surface of the nasopharynx during childhood and in most cases persists asymptomatically into adulthood.[1] Transition from asymptomatic colonization to disease occurs when *S. pneumoniae* migrates to other tissues of the human body. This bacterium often colonizes the lungs being the leading cause of bacterial pneumonia. Colonization of other body tissues may give rise to meningitis, otitis

media, and sepsis. The pneumococcus affects especially young children, the elderly, and immunocompromised individuals. Diseases caused by pneumococci constitute a major public health problem. In 2017, the World Health Organization included *S. pneumoniae* in the list of the 12 priority pathogens that urgently require new antimicrobials. The emergence of antibiotic-resistant strains has conferred this bacterium the status of superbug.

Normal disease progression to the lung or bloodstream exposes *S. pneumoniae* to various stress conditions and fast adaptation to these challenging situations is a crucial step to bacterial survival. Adjusting the RNA amount at the post-transcriptional level ensures a faster and less energy-demanding cell response.[2] Some ribonucleases (RNases) were shown to be effectors in bacterial adaptation and survival under stress.[3] Despite their important roles, knowledge on pneumococcal RNases is still in its infancy, with only a small number of recent studies. RNase R, PNPase and RNase Y were all shown to affect *S. pneumoniae* virulence,[4–6] and RNase YhaM was identified as a stabilizer of noncoding RNAs involved in pneumococcal competence.[6] The present work is focused on RNase R, an exoribonuclease that degrades RNA in the 3′ to 5′ direction in a processive and sequence-independent manner, being the only 3′–5′ exoribonuclease able to degrade RNAs with extensive secondary structures.[7–9] RNase R belongs to the RNase II/RNB family of enzymes, which is present in all domains of life.[7] In *S. pneumoniae* RNase R is the only known member of the RNB family, suggesting a major role in this microorganism. Our work on RNase R has already elucidated interesting roles of this enzyme on the pneumococcal biology. RNase R responds to cold-shock and regulates the expression of the *trans*-translation effector SmpB, which in turn affects RNase R levels.[10] We have also established RNase R as a ribosome dissociation factor, affecting the amount of active translating ribosomes by controlling the level of ribosome dissociation factors. This process has a global impact on protein synthesis and affects cell viability.[11] In addition, our work on the effect of RNase R on *S. pneumoniae* virulence has shown that RNase R interferes with the host immune response, probably by affecting the ability of the pneumococcus to internalize and/or replicate inside *Galleria mellonella* hemocytes.[4]

The overall body of evidence suggests a global role of RNase R on the physiology of this bacterium with repercussions on the *S. pneumoniae* ability to cause infection. Therefore, in this work we have performed a global transcriptomic analysis with RNA sequencing to determine the most significant differences between the *S. pneumoniae* TIGR4 wild type (WT) strain and an isogenic RNase R deletion mutant (Δ*rnr*). The data presented here reveals that RNase R affects the fatty acid biosynthesis transcripts with consequences on the pneumococcal membrane fluidity. We demonstrate that RNase R governs the turnover of transcripts from the fatty acid (FA) biosynthesis pathway, ultimately leading to an unbalanced level of membrane FA in the mutant strain. The implications of the altered membrane FA composition on resistance to several external stresses, such as detergent lysis, oxidative stress and growth under pressure of the antimicrobial peptide nisin, are further explored.

Results

Screening of RNase R-regulated Genes via RNA-Seq

Transcriptomic analysis was performed to better understand how RNase R affects gene expression in *S. pneumoniae* clinical isolate TIGR4. We compared the transcriptome between a Δ*rnr* mutant previously constructed[10,12] and the WT by performing RNA-Seq of total RNA. We only considered transcripts with expression values above 5 RPKM (Reads Per Kilobase Million) and differentially expressed between the two strains more than 1.4-fold (log2FC higher than 0.5). With this approach we found 257 transcripts with relevant differences between the WT and the Δ*rnr* mutant (Table S1 in Supplementary Material). These transcripts were charted in a heatmap to show their normalized expression values and compared between the WT and the RNase R deletion mutant (Figure 1A). Many altered transcripts belonged to the ABC transporter and the phosphoenolpyruvate:carbohydrate phosphotransferase (PTS) functional categories, and the purine biosynthesis pathway seems also to be affected by deletion of RNase R (Figure 1B). Some of these genes were also shown to be altered in unrelated *S. pneumoniae* mutants and growth conditions.[13,14] An enrichment of the transcripts belonging to the fatty acid biosynthesis pathway was also detected. Since fatty acid biosynthesis is considered an attractive antibiotic target,[15] in this work we decided to focus on the fatty acids biosynthesis genes. All the genes required for type II fatty acid biosynthesis, known as the FASII pathway, are located in a single cluster in the *S. pneumoniae* genome, the fab cluster, which is represented in Figure 1C. Our RNA-Seq results show an increased level of most of these transcripts in the absence of RNase R and therefore we investigated the possible involvement of this enzyme in fatty acid biosynthesis.

RNase R modulates the expression levels of the FASII transcripts

The influence of RNase R on the expression levels of the FASII cluster transcripts was further

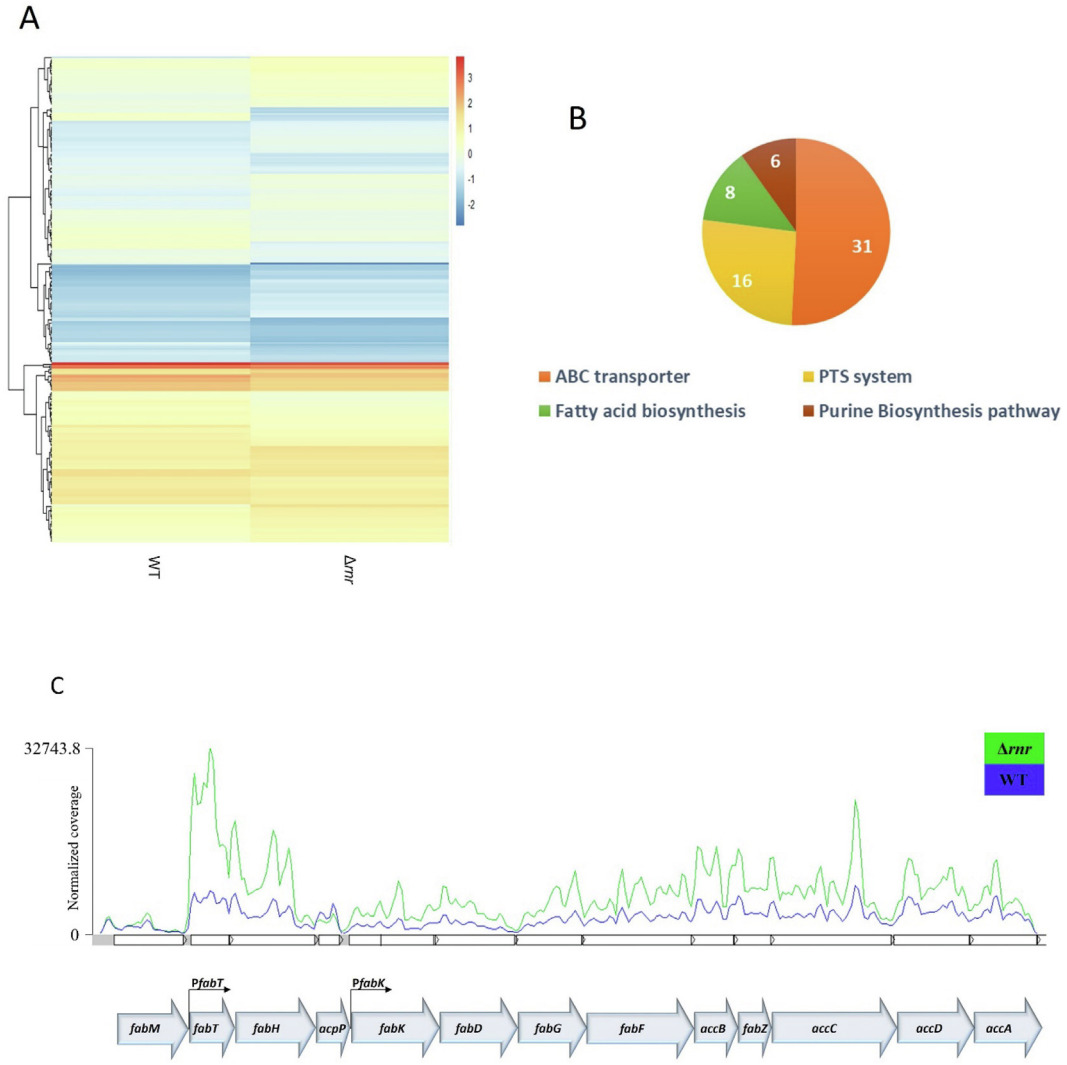

Figure 1. Transcriptomic analysis of RNase R deletion mutant. (A) Heatmap of the transcriptional profile of the 257 transcripts with expression values above 5 RPKM. Hierarchical clustering was done to group genes with similar expression pattern in terms of $\log_2$RPKM. **(B)** Representation of the functional categorization for the transcripts with differences between WT and the Δ*rnr* mutant. **C)** Read coverage plot of the FASII gene cluster. Blue line corresponds to the WT, while green line corresponds to Δ*rnr*. The *y* axis represents the normalized coverage of reads, the *x* axis represents the gene position. The corresponding *fab* genes are represented below. Promoters P*fabT* and P*fabK* control the expression of the FA initiation and elongation modules respectively.

evaluated by Northern blot. We compared the steady-state levels of *fabT*, *fabH*, *fabK*, *fabG* and *fabF* in the WT, the Δ*rnr,* and the complementing Δ*rnr*+R strain. The Δ*rnr*+R strain contains an ectopic copy of the *rnr* gene, rendering RNase R expression levels similar to that of the WT (Supplementary Material, Figure S1). These transcripts were chosen because they showed an increased level in the RNase R deleted strain by RNA-seq, and changes in their expression levels were previously shown to affect the composition of membrane FA.[14,16,17] Two operons have been described within the *fab* cluster: *fab*T-*acp*P and *fabK*-*acc*A, both of which are under the control of the transcriptional regulator FabT.[14,16,18–20] Consistent with these findings, we detected the same-sized transcript when independently using *fabT*- or *fabH*-specific probes. This transcript was accumulated in the strain lacking RNase R compared to the wild type, but not in the Δ*rnr*+R (Figure 2). The transcriptional unit containing these transcripts together with *acpP* was hardly visible when using *fab*T or *fab*H specific probes. The *fabT-fabH-acpP* transcription product was easily detected in a previous publication.[16] This discrepancy might be due to the fact that we used different methods for RNA extraction and worked with the TIGR4 strain, while the previous work was performed with D39. In either case, our results are in agreement with the idea that *acpP* either has its own promoter or its mRNA is

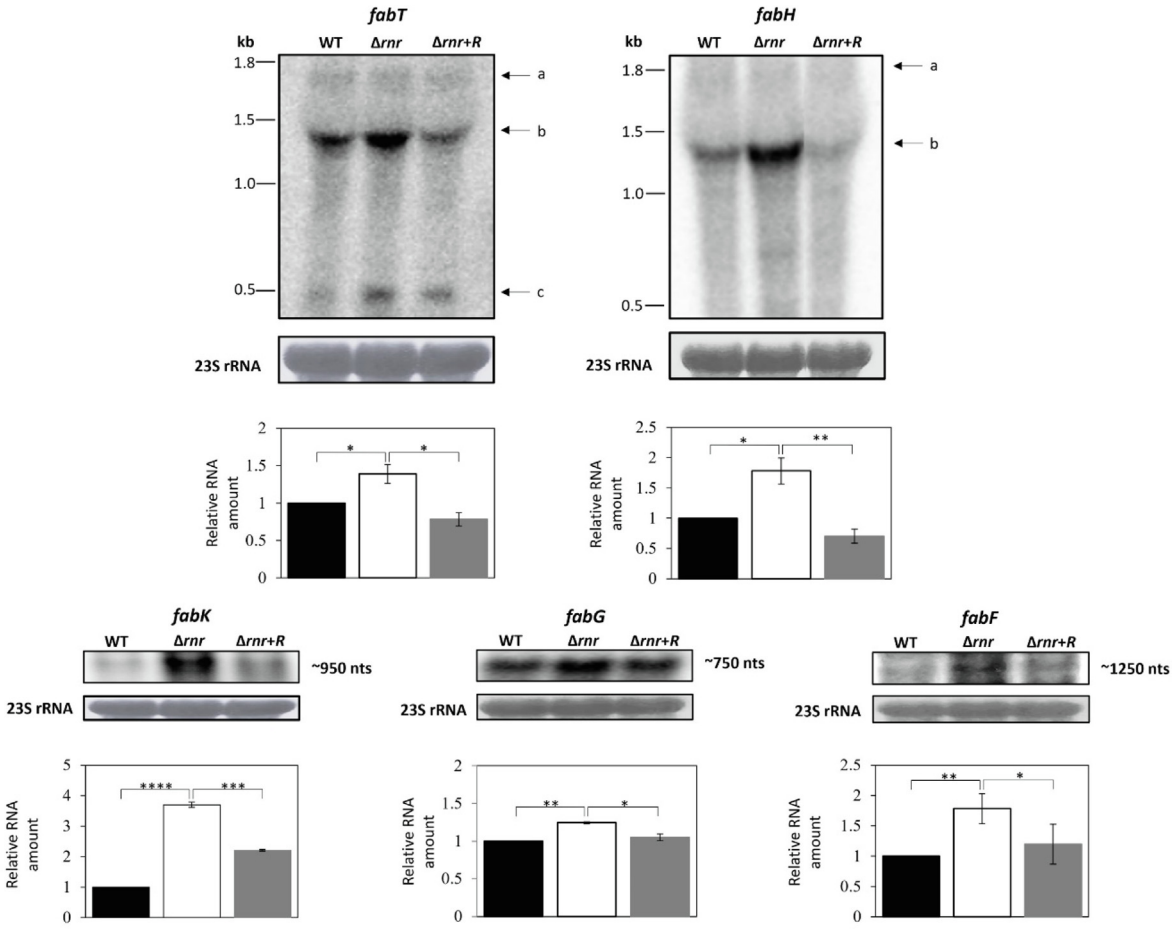

Figure 2. Loss of RNase R leads to accumulation of FASII cluster transcripts. Northern blot analysis of total RNA samples extracted from the WT, RNase R mutant (Δ*rnr*) and Δ*rnr* ectopically expressing RNase R (Δ*rnr*+R). Twenty μg of total RNA were separated on 1.5% agarose gels. Separated RNA molecules were transferred to Hybond-N+ membranes and hybridised with specific probes to FASII transcripts (indicated on top of the images). Loading controls were performed on the same membranes after stripping and probing for 23S rRNA, or by staining the membranes with methylene blue (MB) before hybridization with the probes. Letters a, b and c on the right side of the images indicate the position of the transcriptional units, *fab*T-*fab*H-*acp*P, *fab*T-*fab*H, and *fab*T transcript respectively. Sizes indicated at the left side were inferred according to the molecular weight marker Millennium™ RNA Marker (ThermoFisher Scientific**)**. The bands corresponding to each transcript were quantified and plotted in a bar chart below the respective image. The variation is expressed as fold-change relatively to the expression level in the wild type. These data are representative of three independent experiments (****$p < 0.0001$; ***$p < 0.001$; **$p < 0.01$; *$p < 0.05$).

independently stabilized.[16] The fact that *acpP* levels were not altered in the RNA-Seq results further corroborates this hypothesis. We have also analysed the expression level of *fabM* and confirmed that its level is not affected by the absence of RNase R, as expected from the RNA-Seq results (Figure S2 on supplementary material).

FabT represses the promoter P*fabK*, which is believed to drive the expression of the genes from the second FASII operon (*fabK*-*acc*A), and no other promoters or specific processing sites in this operon have been described.[16] In our conditions, a full-length transcript corresponding to *fabK*-*acc*A was never detected, and all the tested *fab* transcripts from this polycistronic message were found separately. Quantification of the steady-state levels of *fabK*, *fabG* and *fabF* transcripts revealed respectively 3.7, 1.24 and 1.78-fold accumulation in the *Δrnr* strain compared the wild type (Figure 2). Visual inspection of the sequence did not reveal putative transcription terminators, therefore these findings are suggestive of processing events, which would give rise to the individual full-length transcripts detected in our Northern blots.

Accumulation of the steady state levels of *fabT*, *fabH*, *fabK*, *fabG* and *fabF* transcripts observed in the absence of RNase R confirm the RNA-seq results. Furthermore, in all cases the WT levels were partially restored in the complemented strain (Δ*rnr*+R), suggesting a role of RNase R in the

turnover of these mRNAs. To test this hypothesis, we measured the stability of these messages in the WT and in the RNase R mutant. The results of the decay assays are shown in Figure 3A and the respective plots are presented in Figure 3B. In the absence of RNase R all transcripts were

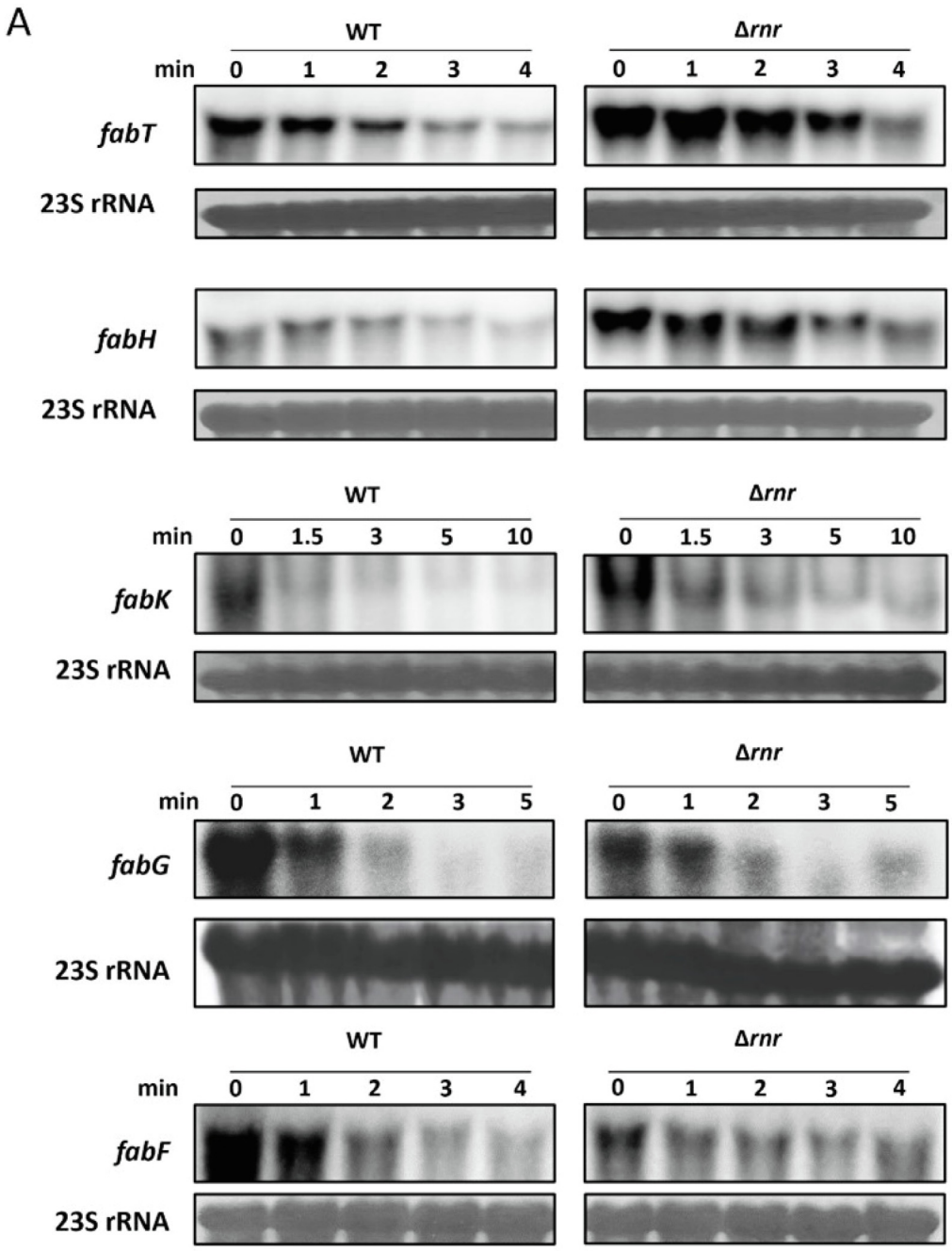

Figure 3. RNase R has a direct role in the turnover of the *fab* transcripts. (A) Northern blot analysis of the stability of the same transcripts in the WT and Δ*rnr*. Transcription was blocked by addition of rifampicin (0 min) and aliquots harvested at the indicated time-points for RNA extraction. Twenty μg of total RNA were separated on 1.5% agarose gels and blotted to Hybond-N+ membranes. Gels were then hybridized with specific riboprobes. Loading controls were performed on the same membranes after stripping and probing for 23S rRNA, or by staining the membranes with methylene blue (MB) before hybridization with the probes. **(B)** Quantification of the corresponding mRNAs was done by scanning densitometry and values of the amount of RNA at zero minutes were considered 100%. The percentage of transcript remaining after rifampicin addition was plotted as a function of time. Decay rates were evaluated by linear regression analysis. Average half-lives (HL) are indicated at the bottom of the corresponding image. Both panels are representative of the results obtained by at least three biological replicates.

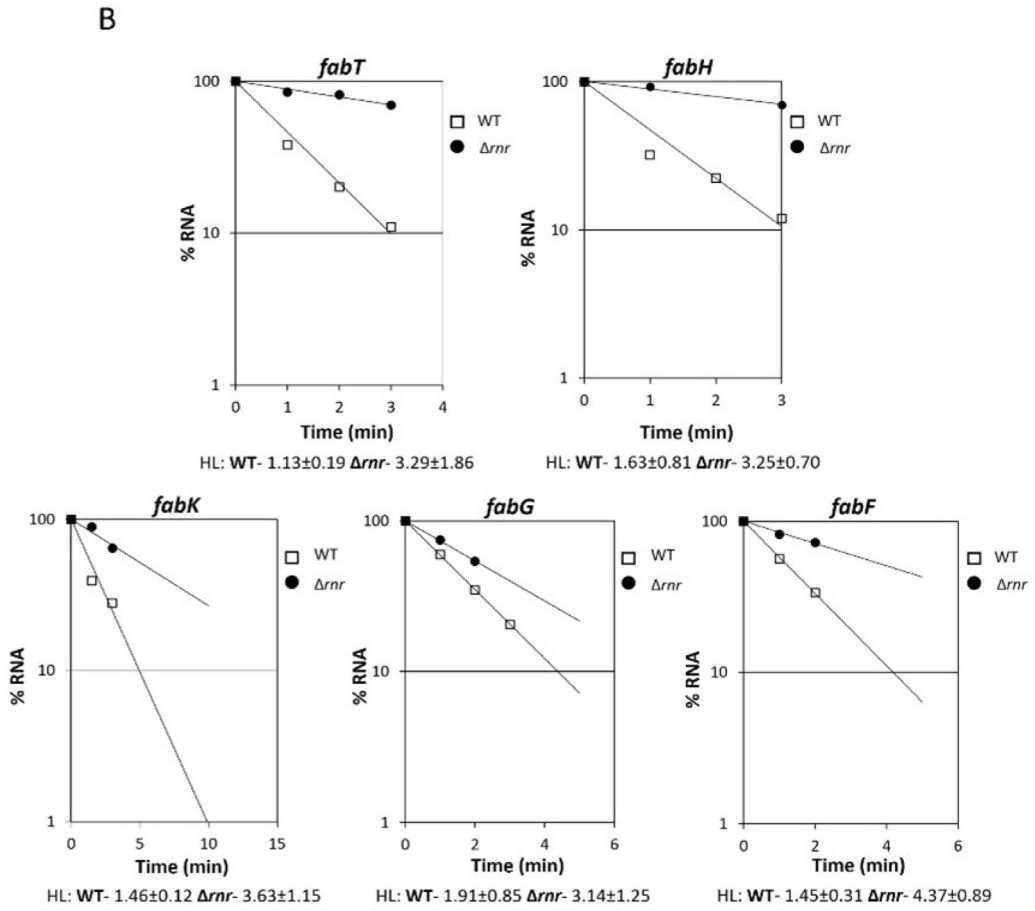

Fig 3. *(continued)*

stabilized, as shown by their higher half-lives in Δ*rnr*. In the WT the half-life of all the messages was below 2 min, whereas in the mutant strain all transcripts had half-lives above 3 min. These results strongly indicate that RNase R is involved in the degradation of the full-length transcripts likely derived from previous processing carried out by other(s) ribonuclease(s). Degradation of these individual messages may involve several ribonucleases and start with an endonucleolytic cleavage, or be immediately degraded from the 3′-end by RNase R. In the RNase R mutant, the presence of PNPase, which is a 3′–5′ exoribonuclease more sensitive to RNA secondary structures, could be one explanation for differential stabilization of these RNAs.

Overall, these data are in agreement with a direct role of RNase R in the turnover of the FASII genes, resulting in higher expression levels in the RNase R lacking strain.

Membrane fatty acid composition is altered in the RNase R deleted strain

Alterations in the expression level of genes from the *fab* cluster have long been known to affect the fatty acid balance leading to abnormal composition of cell membranes.[14,21] Thus, we decided to determine the fatty acid composition of the WT and Δ*rnr* membranes by gas chromatography. As shown in Figure 4A we could observe the presence of the following saturated fatty acids: lauric acid (C12:0), myristic acid (C14:0), palmitic acid (C16:0) and stearic acid (C18:0) in both strains. Regarding unsaturated fatty acids we identified mono-unsaturated FA, including two C16:1 isomers (Δ7 and Δ9), three C18:1 isomers (Δ9, Δ11 and Δ13) and the di-unsaturated FA C18:2, in agreement with the literature.[22,23] Although the total fatty acid content in the mutant cells was similar to the levels measured in the WT (Figure 4B), the Δ*rnr* strain presented alterations in their relative proportions. Mutant cells had lower percentages of C14:0 and C16:0 and increased proportions of all species of C18 FA (C18:0, the three C18:1 isomers, as well as 18:2) (Figure 4A). These changes in individual fatty acids led to alterations in derived parameters related to fatty acid elongation and unsaturation processes, such as the ratio C18/C16 (Figure 4C), which was higher in the mutant, and the proportion of saturated fatty acids (∑Sat) (Figure 4D) which was lower in the same mutant strain. Although small, the differences in FA composition between Δ*rnr* strain and wild type strains were

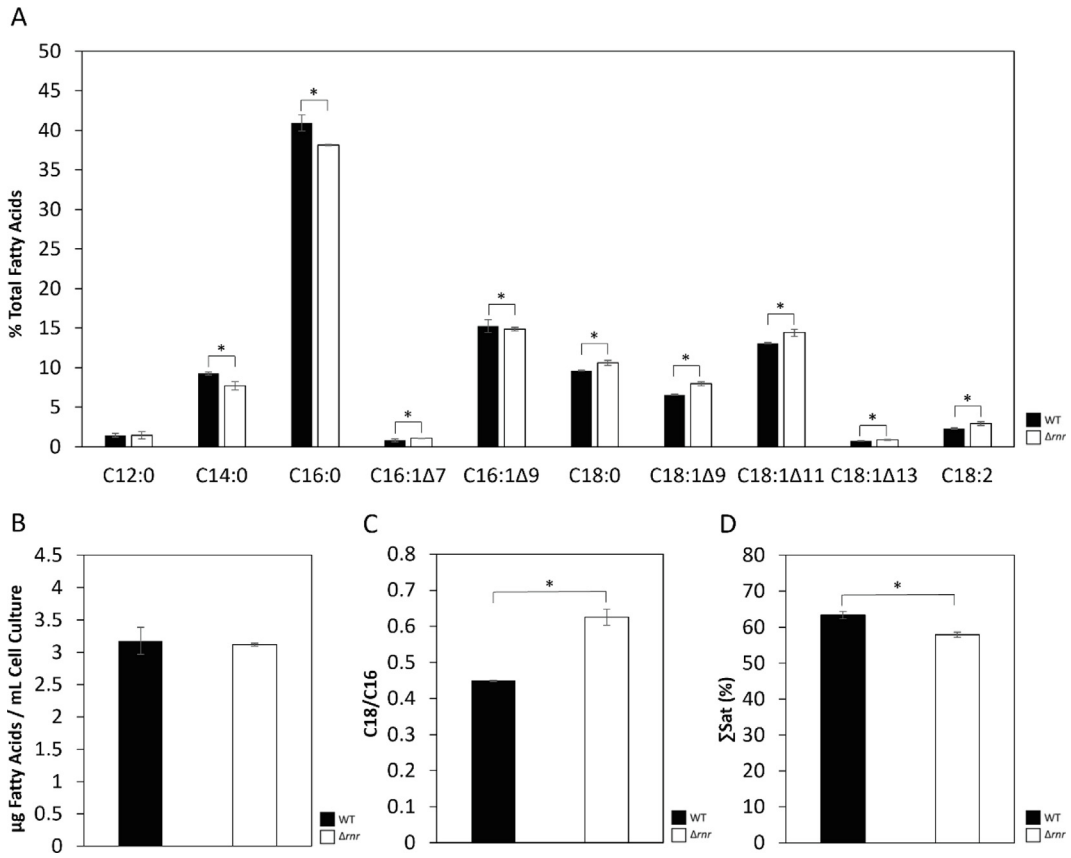

Figure 4. Different composition of membrane fatty acids in WT and Δ*rnr* strains. (A) Fatty acid composition of wild type (WT) and mutant (*Δrnr*) cells of *S. pneumoniae*, expressed as percentage of total fatty acids**. (B)** Total fatty acids contents (expressed in µg FA/mL cell culture). **(C)** Ratio between FA with 18 carbons to FA with 16 carbons. **(D)** Percentage of saturated fatty acids (∑sat). Cultures of *S. pneumoniae* strains were grown to an $OD_{600} \approx 0.3$. Fatty acid methyl esters prepared from bacterial cells were analysed by gas chromatography. Values correspond to average ± standard deviation (*$p < 0.05$). These results were obtained by the analysis of three biological replicates.

significant. Similarly small differences were previously detected upon induction of the response regulator YycF of the YycFG two-component system, in which a 1.58-fold increase of the ratio C18/16 appears to contribute to abnormal septation.[14] Therefore, these results suggest that the increased level of the FASII messages, observed in the absence of RNase R, affects FA biosynthesis, leading to an altered membrane fatty acid composition.

Δrnr is more susceptible to detergent lysis

Composition of the membrane lipid bilayer determines its biophysical properties and affects membrane integrity and permeability.[24] Membrane FA composition is influenced by different stress conditions and has been related to stress tolerance, namely temperature, pH, oxidative stress and detergent lysis.[16,21,23,25,26] We examined the sensitivity of the WT, Δ*rnr,* and Δ*rnr*+R to detergent lysis by measuring tolerance to sodium deoxycholate. Treatment with 2.5% sodium deoxycholate reduced the optical density in Δ*rnr* mutant to 10% after 2.5 min (Figure 5). By contrast, the optical density of wild type and Δ*rnr*+R strains was reduced to ~50% over the same time and was maintained approximately 30–40% at longer times. These results revealed an increased sensitivity of the Δ*rnr* mutant to sodium deoxycholate when compared to the strains containing RNase R. Changes in membrane fluidity caused by the increased expression level of the FASII messages could be the reason for the decreased tolerance to sodium deoxycholate of the RNase R mutant strain.

Resistance to oxidative stress

Bacterial adaptation in response to oxidative stress includes changing the fatty acid composition of the membrane and this is also documented in *S. pneumoniae*.[14,21,23,25] We already know that RNase R is essential to the survival of pneumococci challenged with H_2O_2,[4] and the higher content of unsaturated FA of the Δ*rnr* membrane, is likely to affect cells susceptibility to lipid peroxidation caused by oxidizing agents. Therefore, we studied if the membrane of Δ*rnr* is more prone to lipid peroxidation than the WT membrane. Peroxidation of membrane lipids was analysed in WT, Δ*rnr* and Δ*rnr*+R cells before and

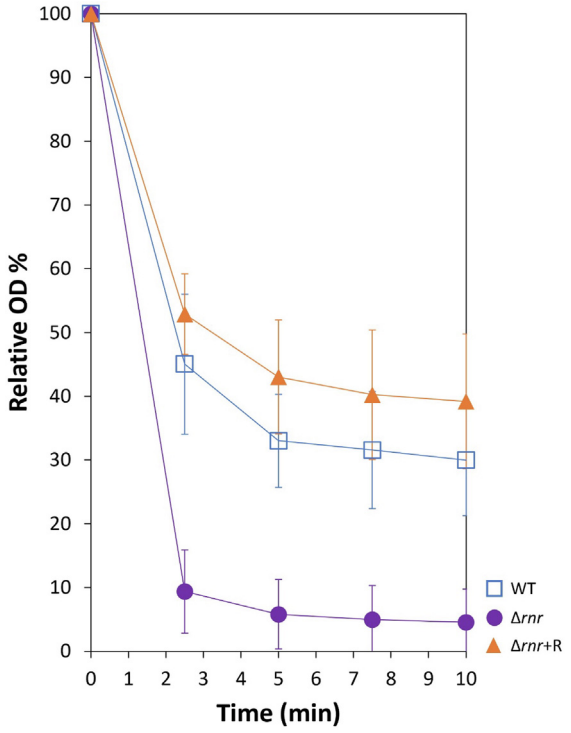

Figure 5. Δ*rnr* strain is more susceptible to lysis by sodium deoxycholate. The figure represents the relative cell density after addition of 2.5% sodium deoxycholate. Wild type (WT), RNase R deleted (Δ*rnr*), and the complemented (Δ*rnr*+R) strains were grown in THY medium, until the beginning of the exponential phase ($OD_{600} \approx 0.3$) and then challenged with 2.5% sodium deoxycholate. The absorbance at 600 nm was monitored for the indicated time-points. The results were normalized to the optical density obtained for the same culture without detergent. These results were obtained from at least three independent assays.

after exposure to H_2O_2 by measuring the production of Thiobarbituric Acid Reactive Substances (TBARS). As expected, the TBARS increased in all the strains after H_2O_2 challenge (Figure 6A). However, the percentage of the lipid peroxidation by-product, malondialdehyde (which reacts with thiobarbituric acid), was significantly higher in the Δ*rnr* mutant (41.89% ± 1.92) than in RNase R containing strains (16.9% ± 5.28 in wild type and 18.1 3% ± 4.37 in Δ*rnr*+R).

In addition, RNase R expression level was increased after H_2O_2 Exposure. Western blot with RNase R specific antibodies, carried out before and after 5 mM H_2O_2 addition, shows about 50% increase in the RNase R level at 30 min post-exposure (Figure 6B). This result provides additional evidence for an important role of RNase R in the adaptive response of the pneumococcus to oxidative stress.

Δrnr is more susceptible to nisin

The antimicrobial peptide nisin exhibits high activity against Gram-positive bacteria and acts by targeting the bacterial membrane. Once there, binding to Lipid II (a precursor molecule in the synthesis of the bacterial cell wall) disrupts its function in cell wall biosynthesis and causes pore formation.[27] Since membrane fluidity has been related with nisin susceptibility,[28] we investigated *S. pneumoniae* growth (WT, Δ*rnr* and Δ*rnr*+R strains) in the presence of this antibiotic. For this, the WT, the Δ*rnr* mutant and the RNase R complemented strain Δ*rnr*+R were cultured with different nisin concentrations (50, 75, 100 and 250 μg/mL) and the respective growth was monitored over 20 h. Growth curves are shown in Figure 7 and the doubling times are shown in Table 1. All the strains presented a longer Lag phase for increasing nisin concentrations. However, the Δ*rnr* mutant grew slower than the RNase R containing strains for concentrations below 100 μg/mL, showing doubling times ~30% higher. At 100 μg/mL the Δ*rnr* growth was completely inhibited, whereas the WT and Δ*rnr*+R were still able to grow. None of the strains could grow at 250 μg/mL. Overall, these results show that RNase R plays a role in the pneumococcus resistance to nisin.

Discussion

Maintaining cytoplasmic membrane integrity is critical for bacterial survival and adaptation to stress conditions, and bacterial response to environmental changes involves adjusting its lipid composition.[29] Modifications in membrane lipid composition result in alterations in membrane biophysical properties, and a correct FA profile is essential for membrane homeostasis[22] (reviewed by 17). In this work we show that RNase R regulates the expression level of several transcripts from the FA biosynthesis pathway, with consequences on the FA composition of *S. pneumoniae* cell membrane, ultimately influencing the stress response ability of this pathogen.

In the FA biosynthesis pathway, membrane fatty acids are produced by a set of enzymes encoded by the genes of the FASII cluster. The initiation enzyme FabH, performs the first condensation reaction on the malonyl-ACP supplied by the concerted action of the multisubunit acetyl-Coenzyme A carboxylase (AccABCD) and the manolyl-ACP transacylase (FabD). The nascent fatty acids are extended by the elongation module two carbons at a time, in a series of repetitive steps performed in *S. pneumoniae* by the enzymes FabG, FabZ, FabK and FabF (reviewed in[17,30]). The end products of the pathway consist primarily of 16- and 18-carbon acyl-ACPs, which can be saturated or unsaturated and compose the

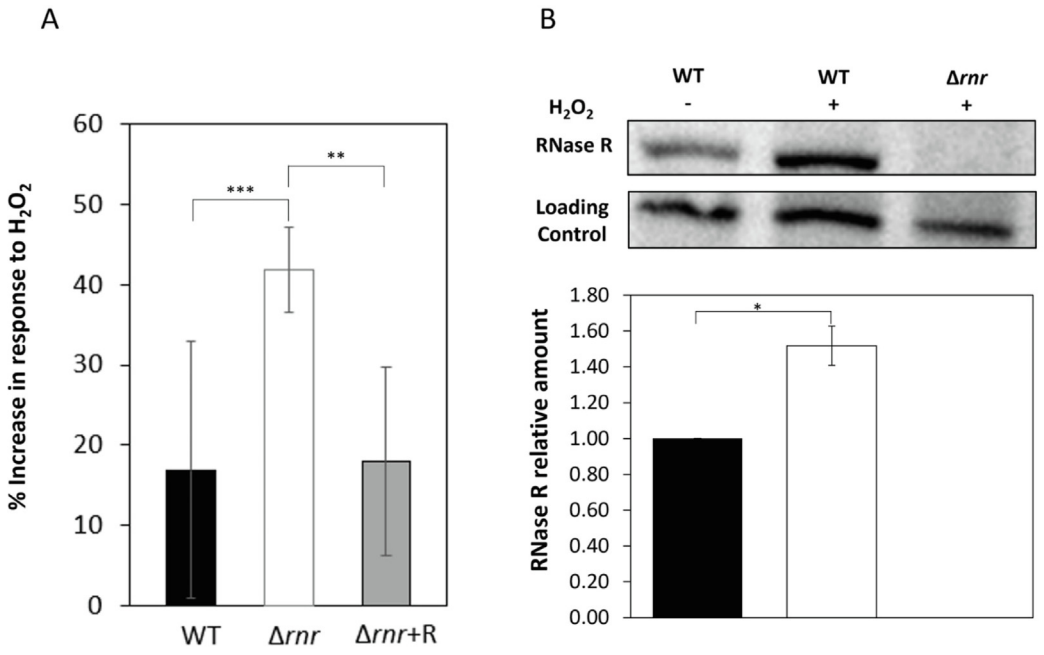

Figure 6. (A) Lipid peroxidation is higher in the RNase R mutant. The figure represents the increased level of lipid peroxidation in response to oxidative stress caused by exposure to H_2O_2 in WT, RNase R mutant (Δ*rnr*) and Δ*rnr* expressing RNase R *in trans* (Δ*rnr*+R). These strains were grown in THY medium, until the beginning of the exponential phase ($OD_{600} \approx 0.3$) and then challenged with 5 mM of H_2O_2. Thiobarbituric acid reactive substances (TBARS) were measured before and after H_2O_2 exposure and the results presented here were normalized to the TBARS obtained for the same culture without H_2O_2. This data is representative of four independent experiments (***$p < 0.001$; **$p < 0.01$). **(B) RNase R levels increase in cultures exposed to H_2O_2.** Expression of RNase R was analysed in the wild type (WT) by Western blot before (−) and after 5 mM H_2O_2 addition (+) as indicated on top of the image. Δ*rnr* mutant was used as negative control. A non-specific band detected with the same antibodies was used as loading control. Total proteins (∼100 μg) were separated in a 7% tricine–SDS-polyacrylamide gel (Haider et al., 2010) and blotted into a nitrocellulose membrane. Immunodetection was performed with RNase R-specific antibodies using Western Lightning Plus-ECL Reagents (PerkinElmer) and the iBright1500 (Invitrogen by Thermo Fisher Scientific) was used to obtain and quantify the images. The amount of RNase R is relative to its expression before stress exposure and is a mean of three replicates (*$p < 0.05$).

hydrophobic portion of the membrane phospholipids. The isomerase FabM introduces the double bond and the unsaturated FA/saturated FA ratio ultimately depends on the competition between FabM and the FabK reductase for the substrate generated by the FabZ dehydratase.[17,31] Our studies showed global stabilization of most of the cognate transcripts in the absence of RNase R, indicating that RNase R is involved in the degradation of these messages, thereby influencing their final amount in the cell.

Transcriptional regulation of the FASII cluster is under the control of FabT, a transcriptional repressor that binds both promoters of the cluster, regulating its own transcription and the expression of all of *fab* genes, except *fabM*.[16,18] However, a putative FabT binding site was also reported upstream of *fabM*[31] and recent works have shown a FabT-dependent regulation of *fabM*.[29,32] Since FabT affinity for DNA is increased by binding to long-chain acyl-ACPs,[18] *fabM* repression was proposed to rely on the formation of highly repressive FabT complexes formed with longer acyl-ACPs.[32] In our case however, the increased levels of *fabT* resulting from RNase R elimination do not seem to affect the expression level of *fabM*. As a repressor, overexpression of FabT was expected to reduce the expression of all the *fab* genes, with the possible exception of *fabM*. In contrast, our observations showed a global increase of the *fab* transcripts in the Δ*rnr* mutant. Since FabT auto-regulates its own expression, the higher levels of the *fabT* transcript in Δ*rnr* could lead to disturbance of the regulatory mechanism. Indeed, our results are in accordance with a previous observation that *fabT* overexpression did not repress *fabK* below the WT levels.[16,21]

Alterations in the expression of these genes are known to result in different fatty acid composition of the membrane phospholipids. Overexpression of all genes from the elongation module were shown to result in longer FA chains.[14,16] The increased levels of transcripts from the elongation module, observed in the RNase R mutant, could

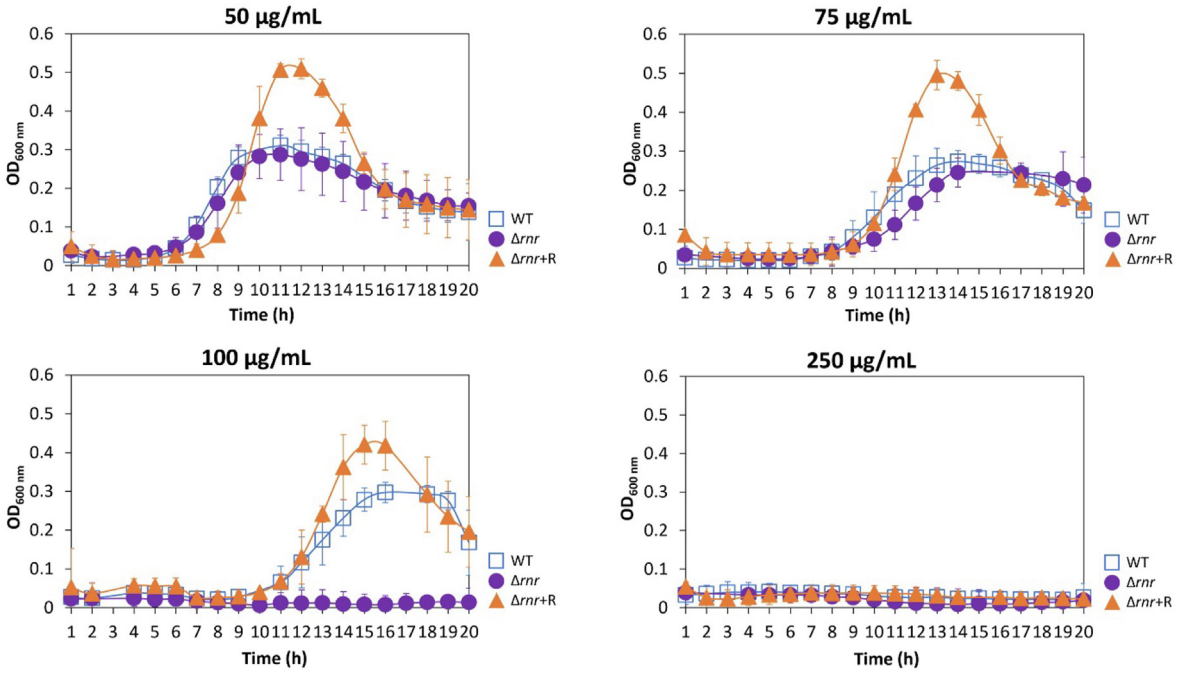

Figure 7. Absence of RNase R leads to increased susceptibility to nisin. Growth curves of wild type (WT), RNase R mutant (Δ*rnr*), and Δ*rnr* ectopically expressing RNase R (Δ*rnr*+R) in several Nisin concentrations (indicated on top of the graphics). WT, Δ*rnr*, and Δ*rnr*+R strains were grown in THY medium, diluted to an OD_{600} of 0.05 in THY containing the indicated range of Nisin concentrations. The absorbance at 600 nm was monitored hourly, for 20 h. The results were normalized to the optical density obtained for the same culture without antibiotic. These results were obtained from at least three independent essays.

Table 1 Doubling time of the Wild type (WT), RNase R mutant (Δ*rnr*), and complementary strain (Δ*rnr*+R) challenged with several nisin concentrations.

Nisin concentrations	Strains		
	WT	Δ*rnr*	Δ*rnr*+R
50 µg/mL	67 ± 5 min	89 ± 10 min	61 ± 7 min
75 µg/mL	76 ± 10 min	99 ± 5 min	61 ± 6 min
100 µg/mL	91 ± 3 min	–	72 ± 8 min

lead to the increased long-chained FA observed in the Δ*rnr* membrane. Notably, FabG and FabF, whose transcripts are stabilized in the strain lacking RNase R, might play a role in the chain length of fatty acids. Overexpression of the essential condensing enzyme FabF was shown to increase the abundance of C18 species as compared to C16,[21] and the FabG reductase is involved in the elongation of FA chains by catalysing the reduction of the carbonyl group from the substrates produced by the condensing enzymes (whether FabH or FabF) (reviewed by 17). Since the length of the fatty acid chain is ultimately determined by the number of cycles of condensation and reduction that occur during the elongation process, increased FabG levels are expected to produce longer-chained FA.

It could be expectable that the global increased expression of the *fab* genes would result in higher amounts of FA. However, we observed similar amounts of total FA in the WT and Δ*rnr* membranes. These results are consistent with the fact that we did not observe variations in the *acpP* level, which encodes the acyl carrier protein (ACP). This protein is a central player in the FASII pathway by carrying all the pathway intermediates, and is fundamental for the fatty acid unit starter production.

Differences in the ratio of unsaturated to saturated FA are determined in *S. pneumoniae* by direct competition between FabM and FabK, and independent overexpression of FabK was previously shown to raise the proportion of saturated FA.[16] Increased levels of *fabK* were also detected in the absence of RNase R but, in our study, we observed higher levels of unsaturated FA. This result might be explained by the fact that several *fab* transcripts were simultaneously elevated in Δ*rnr*, which could influence the amount of available substrate. In fact, Mohedano et al.[14] did not detect higher proportions of saturated FA when several enzymes of the pathway were simultaneously increased.

In *S. pneumoniae*, a significant alteration in the membrane FA profile was related to increasing amounts of endogenous H_2O_2, which were shown to inhibit FabF activity by oxidizing its active site.[23,25] Higher levels of active FabF, observed under anaerobic growth conditions, correlated with

a considerable enhancement in FA unsaturation together with an increase in C18:C16 ratio. Interestingly these results mostly resemble the membrane composition changes observed in Δ*rnr*, which was also characterized by higher proportions of long, unsaturated fatty acyl residues.[23,25] Changes in the pool of membrane lipids in response to transitions between aerobic and anaerobic growth have long been reported to occur in *Staphylococcus aureus*,[33] and the essential pneumococcal regulator YycFG, shown to regulate membrane composition by inhibiting FabT transcription, might also respond to oxygen.[19] We have previously shown that deletion of RNase R strongly affected the capacity of the deleted strain to cope with oxidative stress.[4] Here we show that exogenous H_2O_2 leads to a significant increase in peroxidation of the Δ*rnr* membrane lipids. This increase is in accordance with its higher content in unsaturated FA, which are more vulnerable to oxidizing agents, initiating a chain reaction of lipid damage.[4] The important role of this ribonuclease under oxidative stress is corroborated by the increase in its expression level observed after H_2O_2 challenge. Interestingly our RNA-Seq results showed two genes related to oxidative stress (*Tpx* and *dnaK*) upregulated in Δ*rnr*, and highlighted the effect of RNase R on various transcripts from ABC transporters and PTS systems, whose level was previously shown to change between aerobic and anaerobic growth.[34] The role of RNase R in these processes has still to be investigated.

The higher fluidity of the mutant membrane might also be responsible for the increased sensitivity to detergent lysis observed in the Δ*rnr* strain. Alterations in the membrane homeostasis caused by deletion of *fabT*, were also shown to significantly increase sensitivity to deoxycholate.[16] *fabT* deleted strain also showed an acid-sensitive growth phenotype and pH changes are known to induce alterations in the FA content of the membrane.[16,23,32,35] Loss of RNase R, however, did not increase sensitivity to acidic pH (data not shown).

Additionally, changes in FA composition, particularly those affecting membrane fluidity and rigidity are known to impact the susceptibility of bacteria to nisin-induced membrane disruption.[28,36,37] Importantly, we demonstrate that loss of RNase R impacts the pneumococcal resistance to nisin. The growth defects of Δ*rnr* caused by this membrane-targeting antimicrobial are most likely related to the alteration of the membrane lipid content observed in this strain. The importance of this result is raised by the fact that nisin is an FDA approved GRAS (Generally Regarded As Safe) drug shown to prevent growth of several drug-resistant clinically relevant Gram-positive pathogens including penicillin-resistant *S. pneumoniae*.[38,39] Indeed, the potential utilization of nisin-like peptides to treat bacterial infections has gained clinical interest in the last years. Their low toxicity towards humans together with lower likelihood of bacterial resistance development, compared to many conventional antibiotics, makes them attractive alternative therapeutics.[40,41]

The membrane is an essential component of the bacterial cell, acting as a protective barrier from the external environment. Our data demonstrate that RNase R is directly involved in the turnover of the FASII transcripts, which are accumulated and stabilized in the RNase R lacking strain. The increased level of FASII transcripts results in an altered membrane FA composition. Although small, these changes impact lipid peroxidation, deoxycholate sensitivity, and susceptibility to the antimicrobial peptide nisin, corroborating the connection between RNase R and membrane stress tolerance. The existence of several regulatory mechanisms ensuring the right amount of each enzyme at all times is essential to maintain the proper membrane fluidity. This work identifies RNase R as a major player in the degradation of the FASII transcripts, which in turn determines their levels in the cell, ultimately affecting the FA content of the membrane and conditioning membrane adaptation to stress situations.

Materials and Methods

Bacterial strains, oligonucleotides and growth conditions

S. pneumoniae strains were grown in Todd Hewitt medium, supplemented with 0.5% yeast extract (THY) at 37 °C without aeration, or in THY agar medium supplemented with 5% sheep blood (Thermo Scientific) at 37 °C in a 5% CO_2 atmosphere. When required growth medium was supplemented with 3 μg/mL chloramphenicol (Cm), 1 μg/mL erythromycin (Ery) or 150 μg/mL kanamycin (Km) as specified.

All *S. pneumoniae* strains are isogenic derivatives of the JNR7/87 capsulated strain – TIGR4 and are listed in Table S2 (Supplementary Material).

DNA sequencing was performed at the genomic central service from Centro Nacional de Microbiología (CNM, ISCIII) and oligonucleotide synthesis was performed at CNM, ISCIII and STAB Vida. Oligonucleotide sequences are listed in Table S3 (Supplementary Material).

Construction of Δrnr+R strain of S. pneumoniae

To construct the *Δrnr+R* strain, an ectopic copy of *rnr* gene was introduced into the Δ*rnr* strain chromosome within the *bgaA* locus through allelic replacement.[42] For this purpose, four fragments were generated by PCR (named from 1 to 4). PCR 1 and 4 contained 5′-(coordinates

615828..616648) or the 3′-sequence (620648..621431) of *bgaA* locus and were amplified from the TIGR4 genome using primer pairs BgaA_F/BgaA_Bam and BgaA_Nhe/BgaA_R, respectively. PCR 2 corresponded to the Km resistance cassette and was amplified from pR410 plasmid[43] using primers Km_Bam and Km_Kpn. The PCR 3, containing the *rnr* gene fused to its natural Psec promoter, was amplified from the TIGR4 genome using primers Psec_rnr (harbouring the promoter sequence) and RNR_Nhe. The four PCR fragments were purified, digested with the corresponding restriction enzyme (target sites included in the oligonucleotides), mixed together, and ligated with T4 DNA ligase. A final PCR reaction (PCR 5) was performed using primers BgaA_F2 and BgaA_R2 and the ligation mix as DNA template. The resulting 5075-Kb fragment containing the up sequence of *bgaA*, the Km resistance cassette, the Psec-*rnr*, and the down *bgaA* sequence (Supplementary Material, Figure S3) was used to transform the *Δrnr* as previously described.[44] Transformants were selected with 250 μg/mL Km and positive clones were confirmed by sequencing.

RNase R expression levels in this strain were studied by Western immunoblotting (described below).

RNA extraction from S. pneumoniae cultures

Overnight cultures of *S. pneumoniae* TIGR4 WT and derivatives were diluted in pre-warmed THY to a final OD_{600} of 0.05 and incubated at 37 °C until $OD_{600} \approx 0.3$. 25 mL of culture was collected, mixed with 1 vol of ice cold stop solution (10 mM Tris pH 7.2, 25 mM $NaNO_3$, 5 mM MgCl2, 500 μg/mL Cm) and harvested by centrifugation (10 min, 6000*g*, 4 °C). For mRNA decay studies, transcription was stopped by addition of rifampicin (0.5 mg/mL) and nalidixic acid (20 μg/mL) to growing cells ($OD_{600} \approx 0.3$). At the indicated times, 25 mL of culture was collected, mixed with 1 vol of ice cold stop solution and harvested by centrifugation in the conditions described above. In both cases, total RNA was extracted using Trizol reagent (Ambion) essentially as described by the manufacturer with some modifications as previously described.[11] RNA concentration was estimated using a Nanodrop 1000 machine (Nanodrop Technologies). RNAs used for RNA-Seq were further checked using Bioanalyzer (Agilent) for RNA integrity determination.

Northern blot analysis

For Northern blot analysis, total RNA samples were separated under denaturing conditions by 1.5% agarose MOPS/formaldehyde gel. RNA was transferred to Hybond-N+ membranes (GE Healthcare) by capillarity using 20× SSC as transfer buffer, and UV cross-linked to the membranes immediately after transfer. RNAs integrity and loading control were accessed by staining the membranes in a methylene blue solution (0.03% methylene blue 0.3 M CH_3CO_2Na pH 5.2) and distaining in water. Membranes were then thoroughly washed in 0.5% SDS, 1% SDS and water, and then hybridized in PerfectHyb Buffer (Sigma) for 16 h at 68 °C for riboprobes and 43 °C in the case of oligoprobes. After hybridization, membranes were washed as described.[45] Signals were visualized by Phosphorimager (TLA-5100 Series, Fuji) and analysed using the ImageQuant software (Molecular Dynamics).

Hybridization probes

PCR fragments used as templates for riboprobes were amplified with DreamTaq (Thermo Fisher) and purified using the "PCR Clean-up System" (Macherey-Nagel).

Riboprobe synthesis and oligoprobe labelling were performed as previously described.[45] PCR reactions were carried out using the following primer pairs: smd251/smd252, smd253/smd254, smd075/smd100, smd248/smd249, smd079/smd102 and smd188/smd189 respectively for *fabT, fabH, fabK, fabG, fabF and fabM* specific probes. DNA probe for 23S rRNA was generated using oligonucleotide cbr014, labeled at its 5′-end with [^{32}P]-γ-ATP using T4 Polynucleotide kinase (Thermo Fisher) according to the supplier instructions.

RNA-seq

Total RNA was sent to STAB VIDA (Portugal) for sequencing (Illumina, paired-end, 150 bp, 20 M reads). rRNA was depleted from the samples with the RiboZero kit and sequencing libraries were constructed with the TruSeq kit (Illumina) for bacteria. The quality of the RNA-Seq data was confirmed using the fastQC program. Contaminant adapters and low-quality reads were removed with cutadapt[46] and the remaining reads were mapped against *S. pneumoniae* TIGR4 genome (NC_003028.3, downloaded from NCBI genome database) using Bowtie2 program.[47] Samtools[48] was used to sort the mapping files by genomic position and quantification of RNA-Seq data was performed using FeatureCounts.[49] Transcripts expression was calculated using the RPKM (Reads Per Kilobase per Million mapped reads) normalization method. Differences in expression between the two strains was obtained by calculating the Log_2-Fold change (Log_2FC). Results were filtered to have differences above 0.5 and below −0.5 of Log_2FC and to have RPKM values above 5 in at least one of the samples. Furthermore, all hypothetic proteins were removed from the final analysis.

Fatty acid composition analysis

Overnight cultures of *S. pneumoniae* strains were diluted in prewarmed THY to a final OD_{600} of 0.05 and incubated at 37 °C until $OD_{600} \approx 0.3$. 40 mL of culture were collected, mixed with 1 vol of ice cold stop solution (described above) and harvested by centrifugation (10 min, 6000 × *g*, 4 °C). Bacterial pellets were stored at −80 °C until further analysis.

Fatty acid profiling was performed by direct *trans*-esterification of bacterial pellets in methanol-sulfuric acid (97.5%, v/v) at 70 °C for 60 min, as described in 50 using margaric acid (C17:0) as internal standard. Fatty acid methyl esters (FAMEs) were recovered with petroleum ether, dried under an N_2 flow and resuspended in hexane. One microliter of the FAME solution was analysed in a gas chromatograph (Varian 430-GC gas chromatograph) equipped with a hydrogen flame ionization detector set at 300 °C. The temperature of the injector was set to 270 °C, with a split ratio of 50. The fused-silica capillary column (50 m × 0.25 mm; WCOT Fused Silica, CP-Sil 88 for FAME; Varian) was maintained at a constant nitrogen flow of 2.0 mL min-1, and the oven temperature was set at 190○C. FA identification was performed by comparing retention times with standards (Sigma-Aldrich), and chromatograms were analysed by the peak surface method using the Galaxy software.

Lysis assay with sodium deoxycholate

S. pneumoniae cultures were grown in THY medium to a density of mid-exponential phase and then diluted to $OD_{600} \approx 0.05$. At $OD_{600} \sim 0.3$, bacteria were challenged with 2.5% (v/v) of sodium deoxycholate. OD_{600} of the treated cultures was then followed 2.5, 5, 7.5 and 10 min after sodium deoxycholate addition. As negative control the optical density of the same bacterial cultures without sodium deoxycholate was also monitored.

Thiobarbituric acid reactive substances (TBARS) analysis

Overnight cultures of *S. pneumoniae* strains were diluted in pre-warmed THY to a final OD_{600} of 0.05 and incubated at 37 °C until $OD_{600} \approx 0.3$. At this point half of the bacterial cultures were exposed to 5 mM of H_2O_2. The cultures were further incubated at 37 °C for 30 min without agitation. 25 mL of each culture were then collected, mixed with an equal volume of ice cold stop solution (see above), and harvested by centrifugation (10 min, 6,000 × *g*, 4 °C). Bacteria pellets were stored at –80 °C until further analysis.

The thiobarbituric acid (TBA) reacts with malondialdehyde (MDA), which is an end-product of lipid peroxidation and therefore can be used as a biomarker for lipid peroxidation. The two compounds create a pink-coloured complex that can be measured at 532 nm with a spectrophotometer.

A 0.4% (w/v) TBA solution was freshly prepared in a 10% (w/v) trichloroacetic acid (TCA) solution with ultra-pure water).

The bacteria pellets were resuspended in 1 mL of TBA solution and subjected to sonication for 30 s. The extracts were transferred into glass tubes caped with Teflon lined screw caps and placed in a dry bath at 100 °C for 30 min. After cooling, the tube's contents were transferred to microtubes and centrifuged for 5 min at 15,000 × *g*, 4 °C. Absorbance of the resulting supernatants was measured using an UV–vis spectrometer at wavelengths of 532 nm and 600 nm. Results are expressed as fold change of absorbances (A_{532} nm − A_{600} nm) between extracts from cells exposed to H_2O_2 and the respective non-exposed controls.

Determination of susceptibility to nisin

S. pneumoniae cultures grown overnight were diluted in prewarmed THY to a final OD_{600} of 0.05. Bacterial culture was dispensed on the wells of a 96-well plate containing different concentrations of nisin (50, 75, 100 and 250 μg/mL) prepared in HCl 0.02 N. The plates were incubated without agitation, for 20 h on a Microplate Reader FLUOstar OPTIMA and OD_{600} was measured hourly. The sensitivity to the solvent was tested by monitoring the growth of the same culture incubated with the highest concentration of the solvent, but without antibiotic. As a negative control, the optical density of the same culture without both the antibiotic and the solvent was monitored.

Total protein extraction and Western immunoblotting

Early exponential phase cultures of *S. pneumoniae* TIGR4 WT (OD at 600 nm ≈ 0.3–0.4) were challenged with 5 mM of H_2O_2 and incubated at 37 °C. 20 mL culture samples were collected before and 30 min after stress challenge, mixed with 1 vol of ice cold stop solution (defined above) and harvested by centrifugation (10 min, 6000 × *g*, 4 °C). The cell pellet was resuspended in 100 μL of TE buffer supplemented with 1 mM PMSF, 0.15% sodium deoxycholate and 0.01% SDS. After 15 min incubation at 37 °C, SDS was added to a final concentration of 1%. Protein concentration was determined using a Nanodrop 1000 machine (NanoDrop Technologies). Total protein samples were separated in a modified 7% tricine–SDS-polyacrylamide gel as described.[51]

After electrophoresis, proteins were transferred into a nitrocellulose membrane (Hybond ECL, GE Healthcare) by electroblotting using the Trans-Blot SD semidry electrophoretic system (Bio-Rad). The

membrane was probed with 1:500 dilution of anti-RNase R antibodies.[52] ECL anti-rabbit IgG peroxidase conjugated (Sigma) was used as the secondary antibody in a 1:10000 dilution. Immunodetection was conducted via a chemiluminescence reaction using Western Lightning Plus-ECL Reagents (PerkinElmer).

Statistical analysis

Analysis of the data was performed using GraphPad Prism Software 8.0 for Windows, (San Diego, California USA, https://www.graphpad.com). The results were expressed as mean values of a minimum of three independent experiments ± Standard Errors of the Mean (SEM). The ρ values were calculated using Welch's *t*-test or Kruskal-Wallis test with multiple comparison tests or one-way ANOVA follow-up by a Tukey test with multiple comparisons when appropriate. A value of $p \leq 0.05$ was considered statistically significant in all cases.

CRediT authorship contribution statement

André Filipe Alípio: Writing – review & editing, Validation, Methodology, Investigation, Formal analysis, Data curation. **Cátia Bárria:** Writing – review & editing, Methodology, Investigation, Funding acquisition, Formal analysis, Data curation, Conceptualization. **Vânia Pobre:** Writing – review & editing, Software, Methodology, Investigation, Formal analysis, Data curation. **Ana Rita Matos:** Writing – review & editing, Validation, Supervision, Methodology, Investigation, Formal analysis, Data curation, Conceptualization. **Sara Carrera Prata:** Writing – review & editing, Validation, Methodology, Investigation, Formal analysis, Data curation. **Mónica Amblar:** Writing – review & editing, Validation, Methodology, Investigation, Formal analysis, Data curation, Conceptualization. **Cecília Maria Arraiano:** Writing – review & editing, Investigation, Funding acquisition, Formal analysis, Data curation, Conceptualization. **Susana Domingues:** Writing – review & editing, Writing – original draft, Visualization, Validation, Supervision, Project administration, Methodology, Investigation, Funding acquisition, Formal analysis, Data curation, Conceptualization.

DATA AVAILABILITY

The RNA-Seq data discussed in this publication have been deposited in NCBI's Gene Expression Omnibus and are accessible through GEO Series accession number GSE262258.

DECLARATION OF COMPETING INTEREST

The authors declare that they have no known competing financial interests or personal relationships that could have appeared to influence the work reported in this paper.

Acknowledgments

We are thankful to Teresa Baptista da Silva for technical assistance. Authors acknowledge Eduardo Feijão for assistance with GC and statistical analyses, Luis Morgado for assistance in images preparation and Sandra Viegas for the fruitful scientific discussions.
This research was funded by national funds through FCT—Fundação para a Ciência e a Tecnologia—I. P., Project MOSTMICRO-ITQB with refs UIDB/04612/2020 and UIDP/04612/2020, Projects EXPL/BIA-MOL/1244/2021, BioISI (UID/MULTI/04046/2019), and by project PID2021-124738OB-100 from Ministerio de Ciencia e Innovación of Spain, la Agencia y el Fondo Europeo de Desarrollo Regional (MCIN/AEI/10.13039/501100011033/FEDER, UE). S.D. and V.P. were financed by FCT contracts according to DL57/2016, respectively SFRH/BPD/84080/2012) and (SFRH/BPD/87188/2012). C.B. had a contract under the FCT project PTDC/BIA-BQM/28479/2017.

Appendix A. Supplementary material

Supplementary material to this article can be found online at https://doi.org/10.1016/j.jmb.2024.168711.

Received 11 January 2024;
Accepted 10 July 2024;
Available online 15 July 2024

Keywords:
ribonuclease;
FASII cluster;
fatty acids biosynthesis;
pneumococcus;
stress resistance

† Equal contributors.

References

1. Gray, B.M., Converse, G.M., Huhta, N., Johnston, R.B., Pichichero, M.E., Schiffman, G., Dillon, H.C., (1981). Epidemiologic studies of Streptococcus pneumoniae in infants: Antibody response to nasopharyngeal carriage of types 3, 19, and 23. *J. Infect. Dis.* **144**, 312–318. https://doi.org/10.1093/INFDIS/144.4.312.
2. Silva, I.J., Saramago, M., Dressaire, C., Domingues, S., Viegas, S.C., Arraiano, C.M., (2011). Importance and key events of prokaryotic RNA decay: The ultimate fate of an

RNA molecule. *Wiley Interdiscip. Rev. RNA* **2**, 818–836. https://doi.org/10.1002/wrna.94.
3. Bárria, C., Pobre, V., Bravo, A.M., Arraiano, C.M., (2016). Ribonucleases as modulators of bacterial stress response. *In: Stress and Environmental Regulation of Gene Expression and Adaptation in Bacteria*. John Wiley & Sons, Ltd, pp. 174–184. https://doi.org/10.1002/9781119004813.CH14.
4. Bárria, C., Mil-Homens, D., Pinto, S.N., Fialho, A.M., Arraiano, C.M., Domingues, S., (2022). RNase R, a new virulence determinant of Streptococcus pneumoniae. *Microorganisms* **10**, 317. https://doi.org/10.3390/MICROORGANISMS10020317/S1.
5. Sinha, D., Frick, J.P., Clemons, K., Winkler, M.E., de Lay, N.R., (2021). Pivotal roles for ribonucleases in Streptococcus pneumoniae pathogenesis. *Mbio* **12** https://doi.org/10.1128/MBIO.02385-21.
6. Hör, J., Garriss, G., Di Giorgio, S., Hack, L., Vanselow, J.T., Förstner, K.U., Schlosser, A., Henriques-Normark, B., Vogel, J., (2020). Grad-seq in a gram-positive bacterium reveals exonucleolytic sRNA activation in competence control. *EMBO J.* **39** https://doi.org/10.15252/EMBJ.2019103852.
7. Arraiano, C.M., Andrade, J.M., Domingues, S., Guinote, I. B., Malecki, M., Matos, R.G., Moreira, R.N., Pobre, V., Reis, F.P., Saramago, M., Silva, I.J., Viegas, S.C., (2010). The critical role of RNA processing and degradation in the control of gene expression. *FEMS Microbiol. Rev.* **34**, 883–923. https://doi.org/10.1111/j.1574-6976.2010.00242.x.
8. Chu, L.Y., Hsieh, T.J., Golzarroshan, B., Chen, Y.P., Agrawal, S., Yuan, H.S., (2017). Structural insights into RNA unwinding and degradation by RNase R. *Nucleic Acids Res.* **45**, 12015. https://doi.org/10.1093/NAR/GKX880.
9. Domingues, S., Matos, R.G., Reis, F.P., Fialho, A.M., Barbas, A., Arraiano, C.M., (2009). Biochemical characterization of the RNase II family of exoribonucleases from the human pathogens Salmonella typhimurium and Streptococcus pneumoniae. *Biochemistry* **48**, 11848–11857. https://doi.org/10.1021/BI901105N/SUPPL_FILE/BI901105N_SI_001.PDF.
10. Moreira, R.N., Domingues, S., Viegas, S.C., Amblar, M., Arraiano, C.M., (2012). Synergies between RNA degradation and trans-translation in Streptococcus pneumoniae: cross regulation and co-transcription of RNase R and SmpB. *BMC Microbiol.* **12**, 268. https://doi.org/10.1186/1471-2180-12-268.
11. Bárria, C., Domingues, S., Arraiano, C.M., (2019). Pneumococcal RNase R globally impacts protein synthesis by regulating the amount of actively translating ribosomes. *RNA Biol.* **16**, 211–219. https://doi.org/10.1080/15476286.2018.1564616.
12. Domingues, S., Aires, A.C., Mohedano, M.L., López, P., Arraiano, C.M., (2013). A new tool for cloning and gene expression in Streptococcus pneumoniae. *Plasmid* **70**, 247–253. https://doi.org/10.1016/J.PLASMID.2013.05.005.
13. de Vasconcelos Junior, A.A., Tirado-Vélez, J.M., Martín-Galiano, A.J., Megias, D., Ferrándiz, M.J., Hernández, P., Amblar, M., de la Campa, A.G., (2023). StaR Is a positive regulator of topoisomerase I activity involved in supercoiling maintenance in Streptococcus pneumoniae. *Int. J. Mol. Sci.* **24**, 5973. https://doi.org/10.3390/IJMS24065973.
14. Mohedano, M.L., Overweg, K., De La Fuente, A., Reuter, M., Altabe, S., Mulholland, F., De Mendoza, D., López, P., Wells, J.M., (2005). Evidence that the essential response regulator YycF in Streptococcus pneumoniae modulates expression of fatty acid biosynthesis genes and alters membrane composition. *J. Bacteriol.* **187**, 2357–2367. https://doi.org/10.1128/JB.187.7.2357-2367.2005.
15. Reithuber, E., Nannapaneni, P., Rzhepishevska, O., Lindgren, A.E.G., Ilchenko, O., Normark, S., Almqvist, F., Henriques-Normark, B., Mellroth, P., (2020). The bactericidal fatty acid mimetic 2CCA-1 selectively targets pneumococcal extracellular polyunsaturated fatty acid metabolism. *Mbio* **11**, 1–16. https://doi.org/10.1128/MBIO.03027-20/ASSET/441A54FC-83C3-49C6-B9A1-D4A14711D292/ASSETS/GRAPHIC/MBIO.03027-20-F0005.JPEG.
16. Lu, Y.J., Rock, C.O., (2006). Transcriptional regulation of fatty acid biosynthesis in Streptococcus pneumoniae. *Mol. Microbiol.* **59**, 551–566. https://doi.org/10.1111/j.1365-2958.2005.04951.x.
17. Parsons, J.B., Rock, C.O., (2013). Bacterial lipids: Metabolism and membrane homeostasis. *Prog. Lipid Res.* **52**, 249. https://doi.org/10.1016/J.PLIPRES.2013.02.002.
18. Jerga, A., Rock, C.O., (2009). Acyl-acyl carrier protein regulates transcription of fatty acid biosynthetic genes via the FabT repressor in Streptococcus pneumoniae. *J. Biol. Chem.* **284**, 15364. https://doi.org/10.1074/JBC.C109.002410.
19. Mohedano, M.L., Amblar, M., De La Fuente, A., Wells, J. M., López, P., (2016). The response regulator YycF inhibits expression of the fatty acid biosynthesis repressor FabT in Streptococcus pneumoniae. *Front. Microbiol.* **7** https://doi.org/10.3389/FMICB.2016.01326.
20. Zuo, G., Chen, Z.P., Jiang, Y.L., Zhu, Z., Ding, C., Zhang, Z., Chen, Y., Zhou, C.Z., Li, Q., (2019). Structural insights into repression of the Pneumococcal fatty acid synthesis pathway by repressor FabT and co-repressor acyl-ACP. *FEBS Lett.* **593**, 2730–2741. https://doi.org/10.1002/1873-3468.13534.
21. White, S.W., Zheng, J., Zhang, Y.M., Rock, C.O., (2005). The structural biology of type II fatty acid biosynthesis. *Annu. Rev. Biochem.* **74**, 791–831. https://doi.org/10.1146/ANNUREV.BIOCHEM.74.082803.133524.
22. Aricha, B., Fishov, I., Cohen, Z., Sikron, N., Pesakhov, S., Khozin-Goldberg, I., Dagan, R., Porat, N., (2004). Differences in membrane fluidity and fatty acid composition between phenotypic variants of Streptococcus pneumoniae. *J. Bacteriol.* **186**, 4638. https://doi.org/10.1128/JB.186.14.4638-4644.2004.
23. Pesakhov, S., Benisty, R., Sikron, N., Cohen, Z., Gomelsky, P., Khozin-Goldberg, I., Dagan, R., Porat, N., (2007). Effect of hydrogen peroxide production and the Fenton reaction on membrane composition of Streptococcus pneumoniae. *Biochim. Biophys. Acta Biomembr.* **1768**, 590–597. https://doi.org/10.1016/J.BBAMEM.2006.12.016.
24. Morein, S., Andersson, A.S., Rilfors, L., Lindblom, G., (1996). Wild-type Escherichia coli cells regulate the membrane lipid composition in a “window” between gel and non-lamellar structures. *J. Biol. Chem.* **271**, 6801–6809. https://doi.org/10.1074/jbc.271.12.6801.
25. Benisty, R., Cohen, A.Y., Feldman, A., Cohen, Z., Porat, N., (1801). Endogenous H2O2 produced by Streptococcus pneumoniae controls FabF activity. *Biochim. Biophys. Acta Mol. Cell. Biol. Lipids* **2010**, 1098–1104. https://doi.org/10.1016/J.BBALIP.2010.06.004.
26. Prakash, O., Nimonkar, Y., Shaligram, S., Joseph, N., Shouche, Y.S., (2015). Response of cellular fatty acids to environmental stresses in endophytic Micrococcus spp..

Ann. Microbiol. **65**, 2209–2218. https://doi.org/10.1007/S13213-015-1061-X.
27. Wiedemann, I., Breukink, E., Van Kraaij, C., Kuipers, O.P., Bierbaum, G., De Kruijff, B., Sahl, H.G., (2001). Specific binding of Nisin to the peptidoglycan precursor lipid II combines pore formation and inhibition of cell wall biosynthesis for potent antibiotic activity. *J. Biol. Chem.* **276**, 1772–1779. https://doi.org/10.1074/JBC.M006770200.
28. Badaoui Najjar, M.Z., Chikindas, M.L., Montville, T.J., (2009). The acid tolerance response alters membrane fluidity and induces Nisin resistance in Listeria monocytogenes. *Probiotics Antimicrob. Proteins* **1**, 130–135. https://doi.org/10.1007/S12602-009-9025-8.
29. Zhang, J., Ye, W., Wu, K., Xiao, S., Zheng, Y., Shu, Z., Yin, Y., Zhang, X., (2021). Inactivation of transcriptional regulator FabT influences colony phase variation of Streptococcus pneumoniae. *Mbio* **12** https://doi.org/10.1128/MBIO.01304-21.
30. Zhang, Y.M., Rock, C.O., (2009). Transcriptional regulation in bacterial membrane lipid synthesis. *J. Lipid Res.* **50**, S115. https://doi.org/10.1194/JLR.R800046-JLR200.
31. Marrakchi, H., Choi, K.H., Rock, C.O., (2002). A new mechanism for anaerobic unsaturated fatty acid formation in Streptococcus pneumoniae. *J. Biol. Chem.* **277**, 44809–44816. https://doi.org/10.1074/JBC.M208920200.
32. Eijkelkamp, B.A., Begg, S.L., Pederick, V.G., Trapetti, C., Gregory, M.K., Whittall, J.J., Paton, J.C., McDevitt, C.A., (2018). Arachidonic acid stress impacts pneumococcal fatty acid homeostasis. *Front. Microbiol.* **9**, 813. https://doi.org/10.3389/FMICB.2018.00813/FULL.
33. White, D.C., Frerman, F.E., (1968). Fatty acid composition of the complex lipids of Staphylococcus aureus during the formation of the membrane-bound electron transport system. *J. Bacteriol.* **95**, 2198. https://doi.org/10.1128/JB.95.6.2198-2209.1968.
34. Bortoni, M.E., Terra, V.S., Hinds, J., Andrew, P.W., Yesilkaya, H., (2009). The pneumococcal response to oxidative stress includes a role for Rgg. *Microbiology (n y)* **155**, 4123. https://doi.org/10.1099/MIC.0.028282-0.
35. Fozo, E.M., Kajfasz, J.K., Quivey, R.G., (2004). Low pH-induced membrane fatty acid alterations in oral bacteria. *FEMS Microbiol. Lett.* **238**, 291–295. https://doi.org/10.1111/J.1574-6968.2004.TB09769.X.
36. Li, J., Chikindas, M.L., Ludescher, R.D., Montville, T.J., (2002). Temperature- and surfactant-induced membrane modifications that alter Listeria monocytogenes Nisin sensitivity by different mechanisms. *Appl. Environ. Microbiol.* **68**, 5904. https://doi.org/10.1128/AEM.68.12.5904-5910.2002.
37. Nilsson, L., Chen, Y., Chikindas, M.L., Huss, H.H., Gram, L., Montville, T.J., (2000). Carbon dioxide and Nisin act synergistically on Listeria monocytogenes. *Appl. Environ. Microbiol.* **66**, 769. https://doi.org/10.1128/AEM.66.2.769-774.2000.
38. Aldarhami, A., Felek, A., Sharma, V., Upton, M., (2020). Purification and characterization of nisin P produced by a strain of Streptococcus gallolyticus. *J. Med. Microbiol.* **69**, 605–616. https://doi.org/10.1099/JMM.0.001170/CITE/REFWORKS.
39. Shin, J.M., Gwak, J.W., Kamarajan, P., Fenno, J.C., Rickard, A.H., Kapila, Y.L., (2016). Biomedical applications of Nisin. *J. Appl. Microbiol.* **120**, 1449. https://doi.org/10.1111/JAM.13033.
40. Balciunas, E.M., Castillo Martinez, F.A., Todorov, S.D., Franco, B.D.G. de M., Converti, A., Oliveira, R.P. de S., (2013). Novel biotechnological applications of bacteriocins: A review. *Food Control* **32**, 134–142. https://doi.org/10.1016/J.FOODCONT.2012.11.025.
41. Dischinger, J., Basi Chipalu, S., Bierbaum, G., (2014). Lantibiotics: Promising candidates for future applications in health care. *Int. J. Med. Microbiol.* **304**, 51–62. https://doi.org/10.1016/J.IJMM.2013.09.003.
42. Song, J.H., Ko, K.S., Lee, J.Y., Baek, J.Y., Oh, W.S., Yoon, H.S., Jeong, J.Y., Chun, J., (2005). Identification of essential genes in Streptococcus pneumoniae by allelic replacement mutagenesis. *Mol. Cells* **19**, 365–374. https://doi.org/10.1016/S1016-8478(23)13181-5.
43. Sung, C.K., Li, H., Claverys, J.P., Morrison, D.A., (2001). An rpsL cassette, janus, for gene replacement through negative selection in Streptococcus pneumoniae. *Appl. Environ. Microbiol.* **67**, 5190. https://doi.org/10.1128/AEM.67.11.5190-5196.2001.
44. Acebo, P., Herranz, C., Espenberger, L.B., Gómez-sanz, A., Terrón, M.C., Luque, D., Amblar, M., (2021). A small non-coding RNA modulates expression of Pilus-1 type in Streptococcus pneumoniae. *Microorganisms* **9** https://doi.org/10.3390/MICROORGANISMS9091883.
45. Viegas, S.C., Pfeiffer, V., Sittka, A., Silva, I.J., Vogel, J., Arraiano, C.M., (2007). Characterization of the role of ribonucleases in Salmonella small RNA decay. *Nucleic Acids Res.* **35**, 7651. https://doi.org/10.1093/NAR/GKM916.
46. Martin, M., (2011). Cutadapt removes adapter sequences from high-throughput sequencing reads. *Embnet J.* **17**, 10–12. https://doi.org/10.14806/EJ.17.1.200.
47. Langmead, B., Salzberg, S.L., (2012). Fast gapped-read alignment with Bowtie 2. *Nat. Methods* **9**, 357. https://doi.org/10.1038/NMETH.1923.
48. Li, H., Handsaker, B., Wysoker, A., Fennell, T., Ruan, J., Homer, N., Marth, G., Abecasis, G., Durbin, R., (2009). The sequence alignment/map format and SAMtools. *Bioinformatics* **25**, 2078. https://doi.org/10.1093/BIOINFORMATICS/BTP352.
49. Liao, Y., Smyth, G.K., Shi, W., (2014). featureCounts: An efficient general purpose program for assigning sequence reads to genomic features. *Bioinformatics* **30**, 923–930. https://doi.org/10.1093/BIOINFORMATICS/BTT656.
50. Feijão, E., Gameiro, C., Franzitta, M., Duarte, B., Caçador, I., Cabrita, M.T., Matos, A.R., (2018). Heat wave impacts on the model diatom Phaeodactylum tricornutum: Searching for photochemical and fatty acid biomarkers of thermal stress. *Ecol. Indic.* **95**, 1026–1037. https://doi.org/10.1016/J.ECOLIND.2017.07.058.
51. Haider, S.R., Reid, H.J., Sharp, B.L., (2010). Modification of tricine-SDS-PAGE for online and offline analysis of phosphoproteins by ICP-MS. *Anal Bioanal Chem.* **397**, 655–664. https://doi.org/10.1007/S00216-010-3588-9.
52. Moreira, R.N., Domingues, S., Viegas, S.C., Amblar, M., Arraiano, C.M., (2012). Synergies between RNA degradation and trans-translation in Streptococcus pneumoniae: cross regulation and co-transcription of RNase R and SmpB. *BMC Microbiol.* **12**, 268–282. https://doi.org/10.1186/1471-2180-12-268.